# Composites Prepared by the Anionic Polymerization of Ethyl 2-Cyanoacrylate within Supercritical Carbon Dioxide−Swollen Poly(tetrafluoroethylene-*co*-hexafluoropropylene)

**Edward Kung, Alan J. Lesser,* and Thomas J. McCarthy***

*Polymer Science and Engineering, University of Massachusetts, Amherst, Massachusetts 01003*

*Received April 20, 2000; Revised Manuscript Received July 28, 2000*

ABSTRACT: Supercritical carbon dioxide (SC $CO_2$) was used as an aid in fabricating polymer/polymer composites. Using a two-stage process, ethyl 2-cyanoacrylate (ECA) monomer was anionically polymerized within poly(tetrafluoroethylene-*co*-hexafluoropropylene) substrates. The composite fabrication process involved first infusing triphenylphosphine (the initiator) into the substrate using SC $CO_2$. In the second step, monomer was introduced (again using SC $CO_2$) to the substrate. As the monomer absorbed into the initiator-containing substrate, it polymerized. The composite surfaces were characterized using surface-selective techniques. The mechanical performance of the composites was determined by measuring the adhesive fracture toughness of the composites. The locus of failure of fractured interfaces of composites with epoxy was determined by X-ray photoelectron spectroscopy.

## Introduction

Supercritical carbon dioxide (SC $CO_2$) has been used in the fabrication of polymer−polymer composites. We have demonstrated the viability of infusing monomers into a variety of polymer substrates and subsequently radically polymerizing the monomer within the SC $CO_2$-swollen substrates.[1,2] Polystyrene/polyethylene composites, in particular, showed very interesting phase morphologies that resulted in enhanced mechanical performance when compared to conventional melt-blended systems.[3] Thus far, our research has focused on radical synthesis and bulk characterizations. This paper will discuss research on an anionically polymerized system and the interface properties of the final composites.

The polymerization of functional monomers in the surface region of SC $CO_2$-swollen fluoropolymer substrates allows modification of the surface properties of those substrates, producing composite surfaces. Such a technique is an alternative to the rather harsh and hard-to-control techniques usually employed to modify fluoropolymer surfaces. The introduction of nitrile and ester groups can be effected by the polymerization of cyanoacrylate monomers. Polycyanoacrylates are most commonly synthesized by anionic polymerization, although radical polymerization can also be employed.[4,5] The anionic polymerization of cyanoacrylates is an extremely fast and robust living polymerization. These traits, which will be discussed below, should allow for facile synthesis of the target surface composites. In a $CO_2$ medium, however, an anionic polymerization may be problematic.

$CO_2$ terminates most anionic polymerizations. $CO_2$ is susceptible to nucleophilic attack and will react with anionic initiators or actively propagating carbanions. For most anionic polymerization systems, the resulting carboxylate chain end is normally not reactive enough to continue propagation with monomers or to add to another $CO_2$ molecule (no homopolymerization of $CO_2$ is known to occur).[6] Cyanoacrylate monomers, with electron-withdrawing nitrile and ester substituents, are extremely reactive and can be polymerized by very weak nucleophiles (e.g., amines and phosphines). Anionic cyanoacrylate polymerizations are also known to be extremely difficult to terminate. Pepper investigated the stability of (poly)cyanoacrylate anions by calorimetrically measuring the heat evolved with the successive addition of aliquots of monomer after the additions of potential terminating agents to a living reaction mixture.[4] It was found that the polymerizations of cyanoacrylates are virtually unaffected by the addition of oxygen, water, and $CO_2$. Only the addition of a strong acid (hydrochloric acid) terminated the polymerization.

More recently, Johnston and Pepper studied the stability of polycyanoacrylate anions spectroscopically.[7] The ultraviolet spectrum of a living polycyanoacrylate anion possesses an absorption centered at ∼250 nm. It was found that, upon the addition of $CO_2$ to the reaction mixture, the absorption at 250 nm disappeared nearly instantaneously. This result suggests that $CO_2$ reacts with the cyanoacrylate anion to form a different moiety (presumably a carboxylate anion). Johnston and Pepper did not attempt to identify the carboxylate anion but simply stated that the polymer was nearly instantly terminated by $CO_2$.

The calorimetric data suggest that despite the existence of the terminal carboxylate anions, implied by the spectroscopic data, cyanoacrylate monomer continues to polymerize. For this to occur, either the carboxylate anion decarboxylates and re-forms the cyanoacrylate anion to continue propagation or the carboxylate anion adds to new monomer to continue propagation. Acetate anions are known to initiate polymerization of cyanoacrylates.[8] Scheme 1 shows how either of these two possibilities occur. "I" is a nucleophilic initiator such as an amine or phosphine. If path B occurs, then ester moieties will be incorporated into the backbone of the polymer. This path requires that the kinetics of the cyanoacrylate anion attack on $CO_2$ are competitive with normal homopolymerization (which is known to be very rapid). If the formation of carboxylate anions is competitive, the equilibrium constant (carboxylation−decarboxylation) and the relative rates of paths A and B will dictate which or if both of the two outcomes occur.

Running an anionic polymerization of a cyanoacrylate in fluid carbon dioxide should increase the potential for copolymerization. The increased concentration of $CO_2$

10.1021/ma000695o CCC: $19.00 
Published on Web 10/07/2000

**Scheme 1**

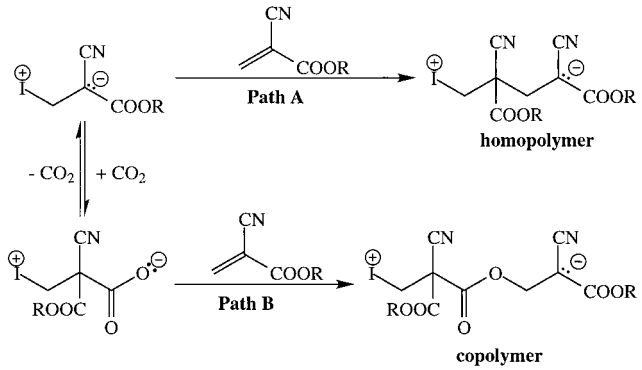


**Scheme 2**

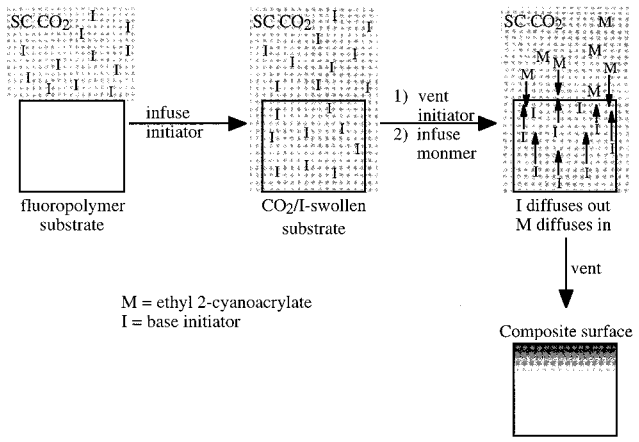


($CO_2$ now being the solvent) should tend to shift the equilibrium shown in Scheme 1 toward the carboxylate anion. Also, increasing the $CO_2$ concentration will increase the probability of a cyanoacrylate anion finding a $CO_2$ molecule to attack before it encounters another cyanoacrylate monomer.

Before we attempted to synthesize polymer composites using cyanoacrylates in SC $CO_2$, we established what product was formed by the anionic polymerization of cyanoacrylates in a $CO_2$ medium. We addressed this issue by examining the polymerization of ethyl 2-cyanoacrylate (ECA) in liquid $CO_2$. Once this issue was resolved, we synthesized composites of poly(ethyl 2-cyanoacylate) (PECA) and poly(tetrafluoroethylene-*co*-helfluoropropylene) (FEP) and characterized the surfaces of the composites.

We modified the technique that had been used for the radical polymerization of styrene within substrates.[1−3] Shown in Scheme 2 is the strategy for synthesizing these composites. First, a polymer substrate is soaked in a SC solution of $CO_2$ containing a nucleophilic intiator (pyridine or triphenylphosphine). Then the system is vented, trapping the initiator within the substrate. The substrate is then introduced to a SC solution of $CO_2$ and ECA monomer. As the monomer is absorbed into the substrate and the initiator begins to desorb from the substrate, the two reactants meet within the upper surface regions of the substrate. As the polymerization proceeds, further outward diffusion of the new polymer does not occur. The resulting product possesses a composite surface. Exactly where within the substrate the secondary polymer forms depends on the relative diffusion rates of monomer into the substrate and initiator out of the substrate.

## Experimental Section

**Materials.** Ethyl 2-cyanoacrylate (ECA) was supplied by Loctite and used without further purification. Poly(tetrafluoroethylene-*co*-hexafluoropropylene) was supplied by DuPont (Teflon FEP 1000A) as 10 mil (nominally) thick sheets. The FEP was cleaned by sonication in HPLC grade tetrahydrofuran (THF) at 60 °C for 24 h. The two initiators, pyridine (anhydrous, 99.8% pure) and triphenylphosphine (99% pure), were purchased from Aldrich. The pyridine was distilled under dry nitrogen from calcium hydride and stored over molecular sieves. The triphenylphosphine was recrystallized three times from ethanol and dried under vacuum. THF (anhydrous, 99.9% pure) that was used for conventional polymerizations was purchased from Aldrich and distilled as needed under nitrogen from purple sodium benzophenone dianion. Carbon dioxide (Coleman grade, 99.99% pure) was purchased from Merriam-Graves and further purified through columns of activated alumina (LaRoche Industries) and a copper catalyst (Engelhard Q-5) to remove water and oxygen, respectively. The $CO_2$ was compressed using a motorized high-pressure screw pump (Isco model 100DM).

**Conventional ECA Polymerizations in THF.** All glassware was base bathed, acid bathed (2.0 M aqueous sulfuric acid), and then thorough washed with clean water and finally dried at 120 °C. All reagent handling and reactions were conducted under a dry nitrogen atmosphere at 23 °C. Using a plastic syringe, an aliquot of ECA monomer was transferred to a glass reaction vessel containing THF. In a separate vessel, an initiator solution of a predetermined concentration of pyridine in THF was prepared. While the monomer solution was vigorously stirred, a predetermined amount of pyridine/THF solution was syringed into the reaction flask. The system was allowed to react for 1 h. The product was recovered by precipitation in acidified methanol and subsequent filtration.

**ECA Polymerizations in Carbon Dioxide.** All reactions were carried out in high-pressure stainless steel vessels. All parts of the vessels were washed in clean acetone, acid bathed (2.0 M aqueous sulfuric acid), then thoroughly rinsed in clean water, and finally dried at 120 °C. Two vessels were used per reaction: a larger reaction vessel (22 mL) and a smaller initiator vessel (8.5 mL). All reactions were conducted at 23 °C. Using a plastic syringe, an aliquot of ECA monomer was transferred to the reaction vessel. This vessel was then sealed and filled with liquid $CO_2$ to a pressure of 102 atm. A predetermined amount of pyridine was transferred to the initiator vessel. This vessel was then sealed and filled with liquid $CO_2$ to 204 atm. The concentrations of the ECA/$CO_2$ and pyridine/$CO_2$ solutions were determined gravimetrically. The two vessels were then connected by a 2 in. long stainless steel nipple. Under vigorous agitation using a vortex mixer, the two vessels were opened, allowing some of the contents of the initiator vessel to flow into the reaction vessel as the pressure difference between the two vessels equilibrated. The two vessels were then closed and separated. The reaction vessel was then weighed to determine the mass of pyridine/$CO_2$ solution transferred into the reaction vessel.

**Polymer Characterization.** $^{13}C$ NMR spectra were recorded in deuterated acetone using a Bruker DPX 300 spectrometer. All chemical shift values are reported in ppm relative to tetramethylsilane. IR spectra were obtained from films solvent-cast on potassium bromide plates using a Bio-Rad FTS 175C spectrometer. The refractive index increment of the PECA in acetone was measured using a Phtal RM-102A differential refractometer. Molecular weights of the polymers were measured using gel permeation chromatography (GPC) through Polymer Laboratories PLgel columns with a Wyatt Technology DAWN DSP-F light scattering detector. Acetone was the GPC solvent.

**Composite Synthesis.** All composite syntheses were carried out in 22 mL high-pressure stainless steel vessels. The vessels were prepared in the same manner described above. The composite preparations required two steps, each using two separate 22 mL vessels. All preparations were conducted at 40 °C.

In the first step (step I), the first vessel (vessel I) was charged with a preweighed sample of FEP and an aliquot of initiator—either pyridine or triphenylphosphine. This vessel was then sealed, tared, and filled with SC $CO_2$ at 40 °C to a pressure of 200 atm. The concentration of the initiator/$CO_2$ solution was determined gravimetrically. Vessel I was then vigorously agitated on a vortex mixer and allowed to soak at 40 °C for 24 h in a heated water bath. At the end of the intiator soak period, the vessel was vented and the FEP specimen removed. The specimen was rinsed throroughly with copious amounts of clean acetone to remove any adsorbed initiator and blown dry with nitrogen. To obtain an approximate mass uptake of the initiator into the FEP, a UV−vis spectrum of the specimen was obtained using a Perkin-Elmer Lambda 2 spectrometer with a virgin FEP specimen as the reference.

In the second step (step II), the specimen was placed in the second vessel (vessel II) along with an aliquot of ECA transferred using a plastic syringe. Vessel II was then sealed, tared, and filled with SC $CO_2$ at 40 °C to 200 atm. The concentration of the monomer/$CO_2$ solution was determined gravimetricallly. Vessel II was then vigorously agitated on a vortex mixer and allowed to soak at 40 °C for various reaction times. At the end of the reaction period, the vessel was vented, and any unreacted monomer leaving the vessel during the venting was noted. The specimen was removed and placed in a vial and allowed to sit for 24 h before any analysis was conducted.

For comparative purposes, pure PECA specimens were prepared on pieces of clean silicon wafers by a vapor deposition technique developed by Woods et al.[9] The silicon wafers were dipped in pyridine and blown dry with nitrogen gas. These substrates were then suspended in a polypropylene container above a pool of ECA monomer that was heated to 40 °C. Within a minute, a relatively uniform layer of PECA forms on the surface of the silicon.

**Surface Characterization.** Surface compositions of the composite specimens were investigated using several surface analytical techniques. Attenuated total reflectance (ATR) IR spectroscopy was performed using a Bio-Rad FTS 175C spectrometer and a 45° germanium ATR element. X-ray photoelectron spectroscopy (XPS) was performed on a Perkin-Elmer-Physical Electronics 5100 spectrometer using Mg Kα X-rays. All XPS data were collected at takeoff angles of 15° and 75° (between the specimen surface and the detector). Advancing and receding contact angles for both water (deionized to 18 MΩ) and hexadecane (Aldrich, 99% pure) were obtained using a Ramé-Hart telescopic goniometer and Gilmont syringes.

**Mechanical Characterization.** The mechanical integrity of the composites was determined by measuring the fracture strength in cleavage of adhesive joints between the composites and metal. The adhesive joints were formed by sandwiching composite specimens between two metal strips coated with epoxy to form double-cantilever beam (DCB) specimens. The epoxy adhesive is a consumer grade epoxy from Devcon (2 Ton Clear) that was prepared and applied in accordance with the recommendations of the manufacturer. The metal beams are stainless steel strips with dimensions 0.307 mm × 12.5 mm × 70.5 mm; they were cleaned with acetone prior to applying the epoxy. The DCB specimens were loaded to failure on an Instron 1123 testing machine fitted with an Instron 2525-807 load cell (±100 N) at a 2 mm/min crosshead speed. From the load-displacement curves, the critical loads for failure and the compliances of the specimens were noted.

## Results and Discussion

**Polymerization in $CO_2$.** The polymerizations conducted in liquid $CO_2$ were precipitation polymerizations. The initial ECA/$CO_2$ solutions, when the systems were observed in a high-pressure view cell, were clear and colorless. The view cell was illuminated to allow observations of the transmitted light. As the polymerizations proceeded, the systems became hazy and changed from colorless to light yellow and then to dark orange in color. Gradually, the hazy orange solution became dark and colorless and filled with large particles that grew in size until the view cell became completely occluded. The color developments are most likely due to scattering effects caused by small polymer particles suspended in the $CO_2$. The final polymer is a fluffy white product.

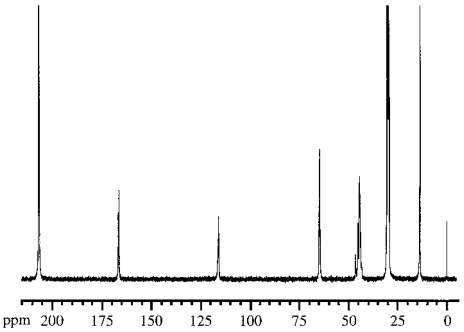


**Figure 1.** $^{13}C$ NMR spectrum of polymer synthesized in liquid $CO_2$ showing clean homopolymerization of ethyl 2-cyanoacrylate.

**Copolymerization?** The IR spectrum of ECA monomer was compared to those of the products formed by polymerizations in THF and $CO_2$. Both products exhibit the loss of vinyl vibrations at 3128 $cm^{-1}$ (asymmetric $sp^2$ $CH_2$ stretching) and 1615 $cm^{-1}$ (C=C stretching). The nitrile vibration at 2246 $cm^{-1}$ (C≡N stretching) is shifted to a slightly higher frequency, and the intensity is decreased due to the loss of conjugation with the vinyl moiety. The product synthesized in THF is expected to be pure homopolymer PECA. By IR, the product formed in $CO_2$ is indistinguishable from the homopolymer prepared in THF.

Figure 1 shows the $^{13}C$ NMR spectrum of the product that was synthesized in $CO_2$. The spectrum matches the spectrum for pure PECA found in the literature with signals at $\delta$ 166 (carbonyl carbons), 115 (nitrile carbons), 44 (main chain methylene and quaternary carbons), 64 (side group methylene carbons), and 14 (side group methyl carbons).[10] If $CO_2$ were incorporated into the main chain of the polymer to any significant extent, separate signals from main chain carbonyl carbons and shifted signals from main chain methylene and quaternary carbons would be expected. The shifted signals would arise from cyanoacrylate monomer units bonded to electron-withdrawing $CO_2$ monomer units. The extremely strong signals at $\delta$ 206 and 30 are due to deuterated acetone. The spectra of products synthesized in THF were identical to that shown in Figure 1. The NMR data concur with the IR results that copolymerization does not occur under the conditions used for synthesis.

**Molecular Weights.** GPC with a light scattering (LS) detector was employed for molecular weight determination. Differential refractometry gave the refractive index increment, d*n*/d*c*, for PECA in acetone to be 0.1159 mL/g. Table 1 summarizes the results of the polymerizations—showing conditions, molecular weights, and yields. Regardless of the solvent employed, unlike truly ideal living anionic polymerizations, the measured molecular weights are much higher than the theoretical values determined by the initial monomer-to-initiator ratio, $[M]_0/[I]_0$. Also, the polydispersity ratios, $M_w/M_n$, are not nearly as narrow as those found in ideal living polymerizations. The results of this investigation agree with the conclusions found by other researchers for

**Table 1. Results of ECA (M) Polymerizations by Pyridine (I) in $CO_2$ and THF at 23 °C**

| no. | solvent | $10^3[I]_0$ (mol %) | $[M]_0/[I]_0$[a] | $10^{-3}M_n$[b] (theor) | $10^{-3}M_n$ (GPC/LS) | $M_w/M_n$ | yield (%) |
|---|---|---|---|---|---|---|---|
| 1 | $CO_2$ | 36.3 | 28 | 3.5 | 670 | 2.0 | 91.4 |
| 2 | $CO_2$ | 26.7 | 38 | 4.7 | 770 | 1.5 | 85.5 |
| 3 | $CO_2$ | 8.3 | 120 | 15.1 | 790 | 1.4 | 89.8 |
| 4 | $CO_2$ | 1.5 | 656 | 82.1 | 1150 | 1.7 | 86.7 |
| 5 | $CO_2$ | 1.2 | 830 | 103.9 | 3490 | 1.3 | 80.0 |
| 6 | THF | 27.4 | 38 | 4.7 | 1780 | 1.2 | 82.8 |
| 7 | THF | 8.4 | 121 | 15.1 | 1880 | 1.6 | 81.4 |

[a] Initial monomer concentration is the same for all reactions, $[M]_0 = 1.0$ mol %. [b] $M_n$(theor) assumes complete initiation, i.e., $= ([M]_0/[I]_0)$(monomer MW).

pyridine-initiated polymerizations of cyanoacrylates and indicate slow and incomplete initiator utilization.[11−14]

**Composite Components.** The virgin FEP specimens used in this study are translucent in appearance/and possess a density of 2.14 g/mL. XPS analysisof the FEP showed that the starting material is clean and consists of approximately 33% carbon and 66% fluorine (F/C = 2) as expected; a spectrum of FEP is displayed in Figure 2. The titanium signal may be from some additive(s) in the polymer. Water contact angles for FEP are $\theta_A/\theta_R$ = 121°/99°; hexadecane contact angles for FEP are $\theta_A/\theta_R$ = 55°/36°.

From XPS analysis, PECA consists of 69% carbon, 20% oxygen, and 11% nitrogen (O/N ≅ 2); a spectrum is displayed in Figure 3. Water contact angles for PECA are $\theta_A/\theta_R$ = 78°/55°; hexadecane contact angles for PECA are $\theta_A/\theta_R$ = 3°/0°. For both water and hexadecane, the contact angles are reasonable for a substrate that contains polar nitrile and ester moieties.

**Composites Using Pyridine as Initiator.** Pyridine was used as one of the initiators and was infused into the FEP substrates during step I of the fabrication technique. The UV spectra for FEP specimens soaked in 2.6 wt % and 0.5 wt % solutions of pyridine in $CO_2$ are shown in Figure 4. Using a literature value for the extinction coefficient of pyridine (1995 L mol$^{-1}$ cm$^{-1}$ at 250 nm),[15] the concentration, *c*, of pyridine loaded into the FEP specimens can be estimated using the Beer−Lambert−Bouguet law. The specimens were 0.0232 cm in thickness. The specimen soaked in the 2.6 wt % solution of pyridine/$CO_2$ had a concentration of approximately 0.022 M (or approximately 0.081 wt %), and the specimen soaked in the 0.5 wt % solution had a concentration of approximately 0.0068 M (or approximately 0.014 wt %).

The specimens soaked in either 2.6 wt % or 0.5 wt % pyridine/$CO_2$ solutions did not produce composites during step II of the fabrication technique. In both cases, the reaction time was 24 h, and after the reaction period, the specimens were found to be encased in a thick layer of foamed PECA. The PECA foam could be peeled off the FEP substrates, and the underlying substrates did not exhibit any change in mass (i.e., no mass uptake of PECA into the FEP). It was concluded that the diffusion of pyridine out of the substrate is much faster than the diffusion of ECA monomer into the substrate and that polymerization occurred completely outside the substrate. All of the monomer was consumed in the "external" polymerization.

**Composites Using Triphenylphosphine as Initiator.** Triphenylphosphine was also used as an initiator and, like pyridine, was infused into the FEP substrates during step I of the fabrication technique. The UV spectrum for a FEP specimen soaked in a 0.9 wt % solution of triphenylphosphine in $CO_2$ is shown in Figure 5. Using the same method as in the pyridine system, the concentration of triphenylphosphine in FEP after step I was estimated. A literature value for the extinction coefficient of triphenylphosphine is 11 000 L mol$^{-1}$ cm$^{-1}$ at 261 nm.[16] The concentration of triphenylphosphine in FEP was appoximately 0.00061 M or approximately 0.0075 wt %.

Unlike the pyridine system, the triphenylphosphine system produced composites in step II. Composites were synthesized using three reaction times: 6, 24, and 49 h. In all cases, the composite specimens were not encased in PECA. The specimens remained translucent although slightly more turbid than virgin FEP. Also, the specimens gained mass and grew in dimension, both due to the uptake of PECA. The incorporation of PECA in FEP increased with increasing reaction time, as is shown in Table 2. Polymerization of monomer in the fluid phase (outside the substrate) did not occur. Polymerization took place only within the FEP substrates.

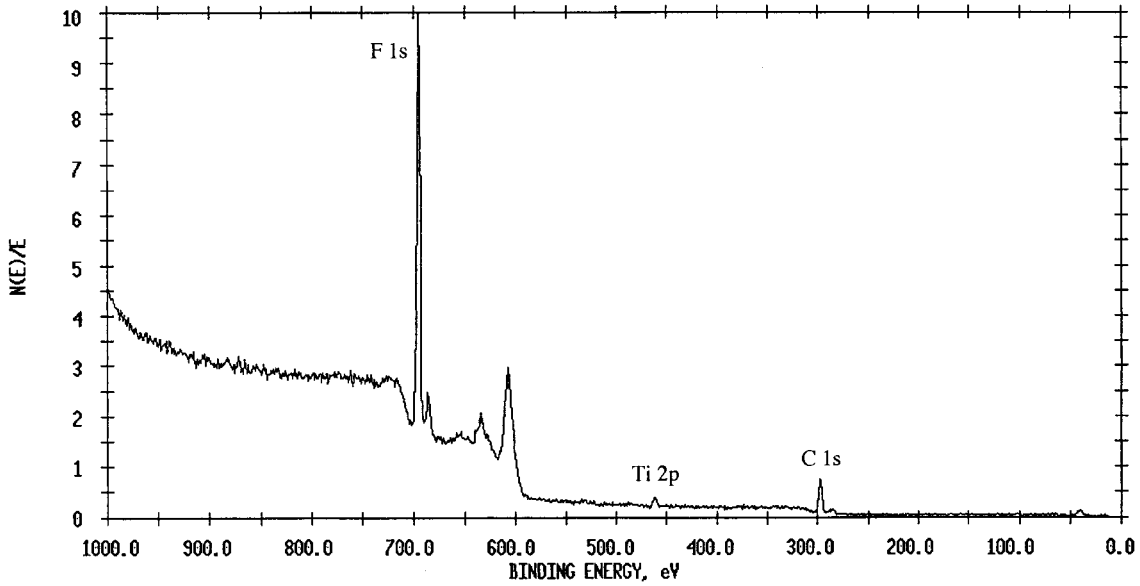


**Figure 2.** XPS spectrum of FEP obtained at a 15° takeoff angle between the specimen and the detector.

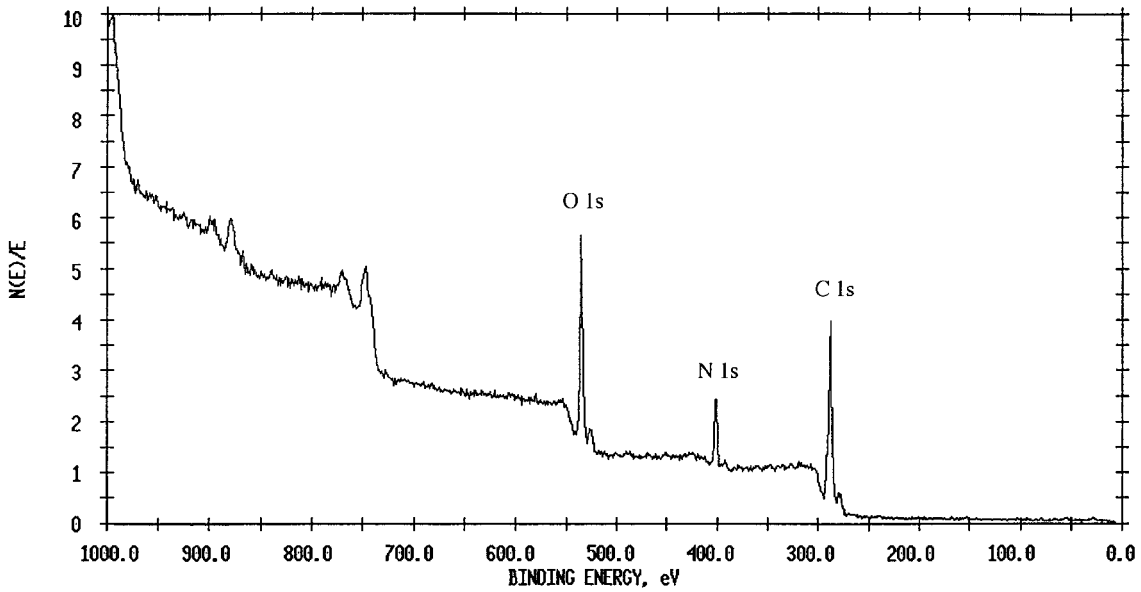


**Figure 3.** XPS spectrum of PECA obatined at a 15° takeoff angle between the specimen and the detector.

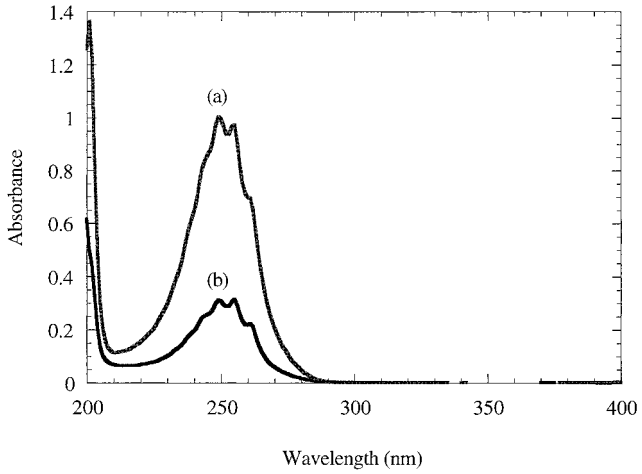


**Figure 4.** UV spectra of FEP specimens soaked in supercritical solutions of pyridine/$CO_2$ at 40 °C and 200 atm for 24 h: (a) soaked in 2.6 wt % pyridine/$CO_2$; (b) soaked in 0.5 wt % pyridine/$CO_2$. Specimens were 0.0232 cm thick.

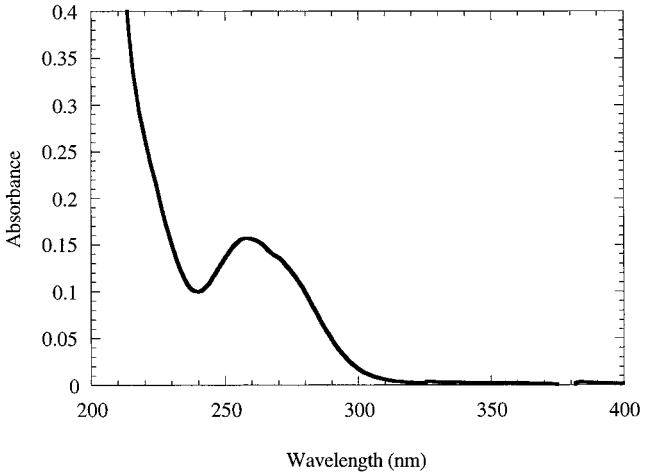


**Figure 5.** UV spectra of a FEP specimen soaked in a supercritical solution of 0.9 wt % triphenylphosphine/$CO_2$ at 40 °C and 200 atm for 24 h. Specimens were 0.0232 cm thick.

Chemical characterization of the surface of the specimens showed that the materials are composites. Comparisons can be made between pure FEP, pure PECA, and the composites. In all subsequent references, the composites are designated PECA/FEP-*X*, where *X* is the reaction time used in step II of the fabrication technique. The ATR IR spectra of virgin FEP, PECA/FEP-24, and PECA/FEP-49 are compared in Figure 6. The XPS spectra for PECA/FEP-24 and PECA/FEP-49 are provided in Figures 7 and 8. The elemental compositions, as determined by XPS, are tabulated in Table 3. The nitrogen, oxygen, and carbon contents increase and the fluorine content decreases with increasing reaction time. The XPS results, however, show a lower content of PECA in the upper 10−50 Å of the specimens compared with the gravimetrically determined compositions shown in Table 2. The hexafluoropropylene comonomer content in FEP is generally 10−12 wt %.[17] Assuming that the FEP material is made up of 12 wt % hexafluoropropylene, then the chemical formula for an average FEP repeat unit is $C_{2.075}F_{4.150}$ with a (repeat unit) molar mass of 103.77 g/mol. The chemical formula for a PECA repeat unit is $C_6H_7NO_2$ with a molar mass of 125.13 g/mol. Using the nitrogen and fluorine concentrations determined by XPS and the chemical formulas of the repeat units of the component polymers, the mass compositions of the specimens within the sampling depth of the XPS experiments can be calculated. These surface mass compositions are tabulated in Table 4.

**Table 2. Mass Uptake and Composition of PECA into FEP as a Function of Reaction Time for the Triphenylphosphine System**

| reaction time (h) | mass uptake (%) | composition (wt %) |
|---|---|---|
| 6 | 19.4 | 16.3 |
| 24 | 31.2 | 23.8 |
| 49 | 69.9 | 41.1 |

Contact angle data are tabulated in Table 5. As might be expected, PECA-24 is more like FEP than PECA/FEP-49. The advancing water contact angle is higher for the composite specimens than pure FEP. This indicates a mixed hydrophobic (FEP) and hydrophilic (PECA) surface. As the water droplet is advanced over hydrophilic domains, the contact line pins causing the contact angle to increase above the pure hydrophobic (FEP) value. The receding water angle also shows pinning and is lower than the pure FEP value, indicat-

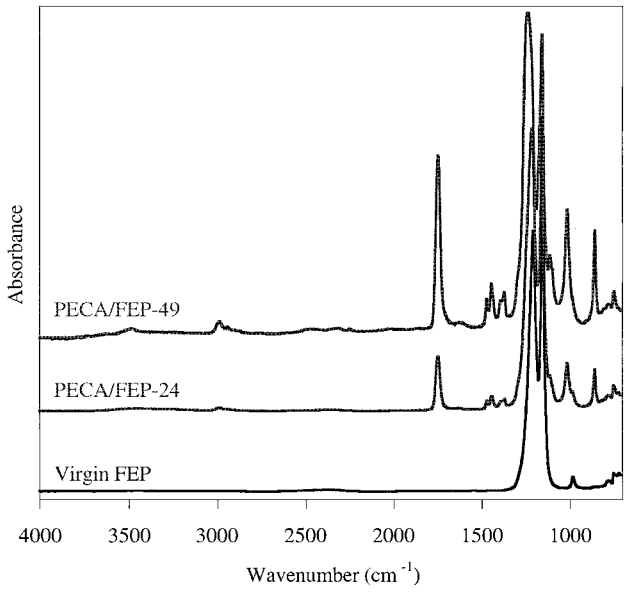


**Figure 6.** ATR IR spectra comparing a composite synthesized for 49 h (top), a composite synthesized for 24 h (middle), and virgin FEP (bottom). A 45° germanium crystal was used as the ATR element.

ing that the composites possess a slightly more hydrophilic surface. The hexadecane results concur with the water results.

PECA/FEP-24 specimens were both rinsed briefly in acetone and subjected to an extensive extraction in THF. The extraction involved sonicating a specimen in THF at 60 °C for several days. The specimens were then analyzed gravimetrically and with XPS. By XPS, the surfaces of the specimens showed a significant loss of PECA (Table 6). However, gravimetrically, the specimens lost only a few fractions of a percent in weight. The PECA is washed from the surface of the specimens, but the solvent resistance of FEP prevents the extraction of PECA from within the bulk of the specimens. Certainly, a great deal of the PECA is located below the surface of the specimens. To what depth the PECA is incorporated and how it is distributed are not known.

**Mechanical Performance.** The fracture strength in cleavage of the DCB specimens can be described by the opening mode fracture toughness, $G_q$. This is a measure of the energy to propagate a crack (create new crack surface area) assuming linear elasticity and is calculated by

$$G_q = \frac{P_q^2}{2B}\left(\frac{\mathrm{d}C(a)}{\mathrm{d}a}\right) \tag{1}$$

where $B$ is the beam thickness (0.307 mm), $P_q$ is the critical load at failure, and $C(a)$ is the specimen compliance as a function of $a$, the crack length.[18] The use of metal beams in the DCB geometry allows the compliance of the test specimens to be dominated by the compliance of the metal beams. A schematic of the test specimen is shown in Figure 9.

The metal beams must be calibrated to obtain their compliance as a function of crack length. DCB test specimens can be simulated by clamping the metal beams together and measuring their compliance at various clamped distances from the loaded ends (thus simulating different crack lengths). From this curve, the compliance as a function of crack length and the derivitave of the compliance with respect to crack length can be determined. This curve can be used to back-calculate the starting crack length of the test specimens once the compliance of the test specimen is measured, because the compliance of the metal beams dominates the compliance of the test specimen. This back calculation requires the use of an iterative numerical method, but that is a trivial problem for modern computers.

The specimens behave linear elastically until a critical load is achieved, after which the specimen fails by cleavage between one of the metal beams and the specimen. From the slope of the specimen's load−displacement curve, the compliance of the specimen can be determined, which in turn provides the crack length and the derivative of compliance with respect to crack length. This and the measured critical load allow the calculation of fracture toughness. The locus of failure was determined to differentiate whether cleavage occurs within the specimen, at the specimen−epoxy interface,

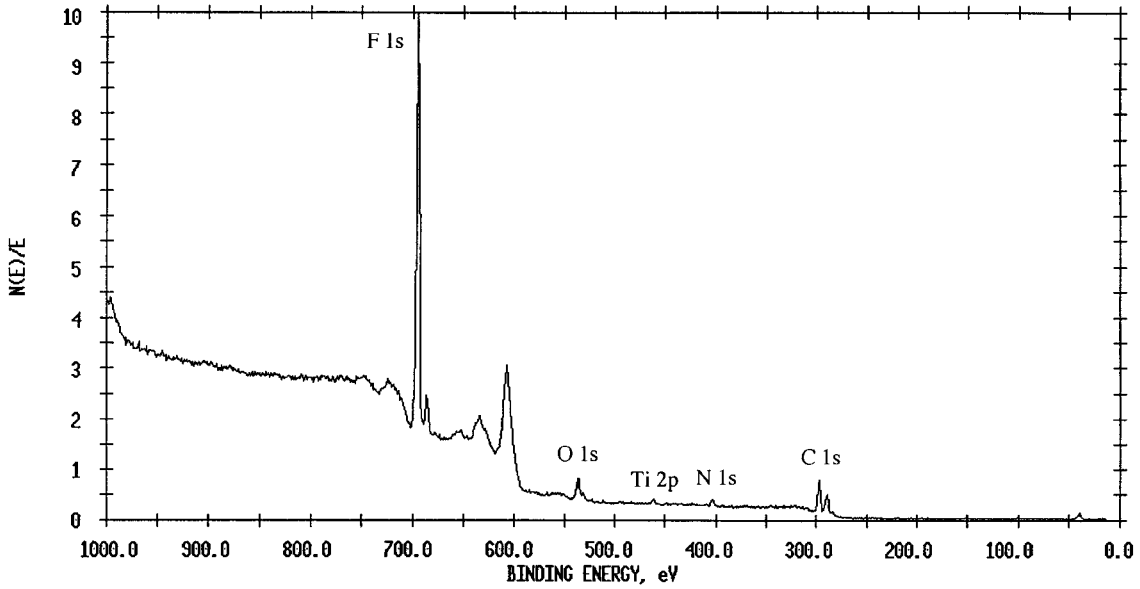


**Figure 7.** XPS spectrum of a PECA/FEP composite specimen synthesized for 24 h (PECA/FEP-24) obtained at a 15° takeoff angle between the specimen and the detector.

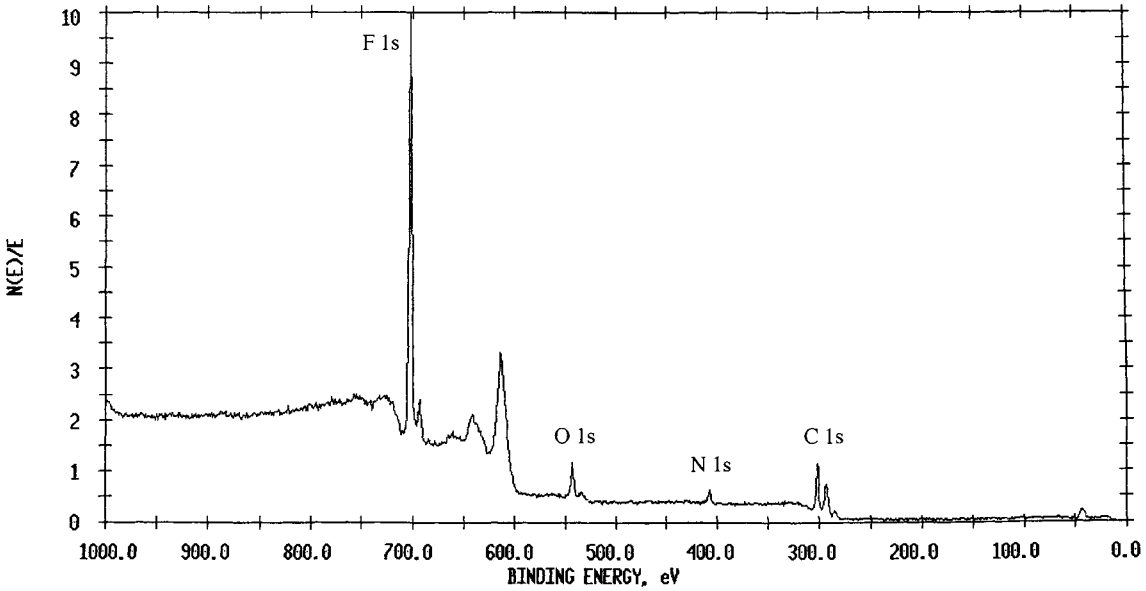


**Figure 8.** XPS spectrum of a PECA/FEP composite specimen synthesized for 49 h (PECA/FEP-49) obtained at a 15° takeoff angle between the specimen and the detector.

**Table 3. XPS Atomic Composition Data for FEP/PECA Composite Surfaces**

| sample | takeoff angle (deg) | atomic concentration C (%) | F (%) | O (%) | N (%) | Ti (%) |
|---|---|---|---|---|---|---|
| FEP | 15 | 33.5 | 65.2 | | | 1.3 |
| | 75 | 33.0 | 65.7 | | | 1.3 |
| PECA | 15 | 69.2 | | 20.7 | 10.1 | |
| | 75 | 68.8 | | 20.2 | 11.0 | |
| PECA/FEP-24 | 15 | 42.1 | 47.5 | 6.7 | 3.3 | 0.4 |
| | 75 | 37.0 | 56.9 | 3.7 | 1.8 | 0.5 |
| PECA/FEP-49 | 15 | 45.2 | 41.6 | 9.0 | 4.2 | |
| | 75 | 43.2 | 46.4 | 6.7 | 3.7 | |

**Table 4. Mass Composition of the Surface of PECA/FEP Composites As Determined from XPS Data**

| sample | takeoff angle (deg) | composition as determined from N and F data (wt % PECA) |
|---|---|---|
| PECA/FEP-24 | 15 | 25.8 |
| | 75 | 13.7 |
| PECA/FEP-49 | 25 | 33.6 |
| | 75 | 28.5 |

**Table 5. Dynamic Contact Angle Data for FEP/PECA Composite Surfaces**

| sample | probe fluid | contact angles $\theta_A$ (deg) | $\theta_R$ (deg) |
|---|---|---|---|
| FEP | water | 121 | 99 |
| | hexadecane | 55 | 36 |
| PECA | water | 78 | 55 |
| | hexadecane | 3 | 0 |
| PECA/FEP-24 | water | 122 | 86 |
| | hexadecane | 52 | 18 |
| PECA/FEP-49 | water | 133 | 83 |
| | hexadecane | 46 | 15 |

within the epoxy or at the epoxy−metal interface. XPS was employed when the locus of failure was not visually obvious. If failure appeared to occur at the specimen−epoxy interface, then both sides of the interface were examined using XPS. The chemical composition of the cleaved surfaces gives an indication of where the failure actually occurred.

Table 7 lists the adhesive fracture toughness of various specimens tested, and Table 8 lists the XPS data used for the failure locus determinations. FEP, as is expected, forms a very weak bond with epoxy. XPS reveals that failure occurs cohesively within the FEP specimen, as is evidenced by the fluorine content at the surface of the epoxy side. Unfortunately, the PECA/FEP-24 composites also form very weak bonds to the epoxy. The toughness values for FEP and PECA/FEP-24 are identical. The failure locus XPS data show that, like FEP, the PECA/FEP-24 composites also fail cohesively within the specimen. The failure locus data provides a hypothesis for the poor bonding behavior of both samples. It is not the lack of adhesion between FEP and epoxy that causes the poor performance, rather it is FEP's cohesive weakness that cause easy failure in adhesion tests. The PECA/FEP-24 composite is predominantly FEP in composition and also fails as though

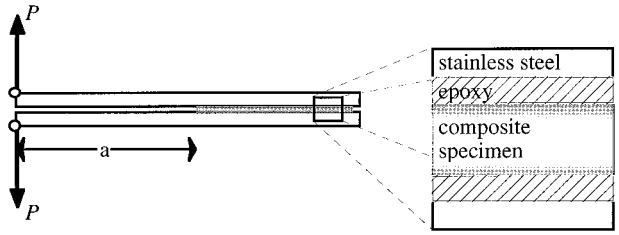


**Figure 9.** Schematic representation of a double-cantilever beam adhesive test specimen.

**Table 6. XPS Atomic Composition Data for PECA/FEP-24 Specimens That Were Rinsed in Acetone or Extracted in Tetrahydrofuran**

| treatment | takeoff angle (deg) | atomic concntration C (%) | F (%) | O (%) | N (%) | Ti (%) |
|---|---|---|---|---|---|---|
| none | 15 | 42.1 | 47.5 | 6.7 | 3.3 | 0.4 |
| | 75 | 37.0 | 56.9 | 3.7 | 1.8 | 0.5 |
| rinsed in acetone | 15 | 39.4 | 58.0 | 2.0 | | 0.7 |
| | 75 | 37.4 | 61.1 | 0.8 | | 0.8 |
| extracted in THF | 15 | 40.9 | 57.2 | 1.2 | | 0.7 |
| | 75 | 37.0 | 61.5 | 0.8 | | 0.8 |

**Table 7. Adhesive Fracture Toughness Data**

| sample | adhesive fracture toughness, $G_q$ (kJ/m$^2$) |
|---|---|
| FEP | $0.00051 \pm 0.00012$ |
| PECA/FEP-24 | $0.00051 \pm 0.00011$ |
| PECA/FEP-49 | $0.00452 \pm 0.00078$[a] |

[a] Mixed failure between specimen−epoxy and metal−epoxy interfaces.

**Table 8. XPS Atomic Composition Data of the Two Sides of Cleaved DCB Test Specimens Where Failure Occurred at the Specimen−Epoxy Interface**

| sample and side | takeoff angle (deg) | atomic concentration C (%) | F (%) | O (%) | N (%) | Ti (%) |
|---|---|---|---|---|---|---|
| virgin | 15 | 80.0 | | 11.0 | 9.0 | |
| cured epoxy | 75 | 77.7 | | 12.3 | 10.0 | |
| FEP | 15 | 35.4 | 64.4 | | | 0.2 |
| specimen side | 75 | 37.7 | 62.1 | | | |
| FEP | 15 | 67.8 | 18.3 | 11.3 | 2.7 | 0.2 |
| epoxy side | 75 | 71.1 | 9.1 | 16.2 | 3.6 | |
| PECA/FEP-24 | 15 | 42.6 | 53.1 | 3.5 | | 0.8 |
| specimen side | 75 | 36.4 | 61.6 | 1.1 | | 0.9 |
| PECA/FEP-24 | 15 | 70.1 | 13.9 | 12.5 | 3.5 | |
| epoxy side | 75 | 71.4 | 9.8 | 13.7 | 5.1 | |

it was pure FEP. Note (Table 8) that no nitrogen is observed in the XPS spectrum of the FEP side of the interface after failure. This indicates failure at FEP-rich regions of the composite. This weak cohesive performance of FEP may be a bulk property or evidence of a "weak boundary layer".

In contrast to PECA/FEP-24, PECA/FEP-49 shows an order of magnitude improvement in the adhesion tests. The failure locus was determined by eye. Visually, one could see patches of the specimen where epoxy remained bonded and other areas where the specimen was visible. The PECA/FEP-24 results suggest that adding polar groups to the FEP surface is not necessary to improve adhesive performance. What is needed, is a method of strengthening the cohesive performance. The higher incorporation of PECA in the PECA/FEP-49 specimens may have provided that strengthening.

## Conclusions

The anionic polymerization of ECA in a $CO_2$ medium was attempted and determined to be viable: the anionic polymerization of ECA proceeds effectively to completion in liquid $CO_2$. Although $CO_2$ is susceptible to nucleophilic attack, $CO_2$ is not incorporated into the final polymer product to any measurable extent under the conditions used in this study. Reducing the temperature of the system and diluting the ECA monomer concentration may yield copolymer; however, neither of these experiments were attempted in this work. Generally, the polymerization results in $CO_2$ compare quite well to polymerizations found in the literature with amine initiators in conventional solvents. The high reactivity of cyanoacrylate monomers toward anionic polymerization is derived from the two electron-withdrawing substituents; other monomers with two electron-withdrawing substiuents may anionically polymerize in $CO_2$ as well.

Using the composite synthesis method described in Scheme 2, it is possible to produce composites of PECA and FEP. The goal of producing a composite at the surface of the FEP substrate was only partially achieved when triphenylphosphine was used as the initiator. The amount of PECA incorporated into the substrate could easily be varied by controlling the time that the initiator-containing substrate was allowed to soak in the ECA/$CO_2$ solution. With longer soak times, more monomer was absorbed into the substrate and incorporated with the existing living PECA. Surface analysis showed that the surface of the substrate was indeed a mixture of PECA and FEP. However, gravimetric analysis and extraction experiments showed that the majority of the PECA was located below the surface. The ECA monomer diffuses into the substrate faster than triphenylphosphine can diffuse out. The location of the polymerization is thus below the surface.

The surface composite fabrication technique investigated here was not optimized. Pyridine diffuses out of the substrate much faster that triphenylphosphine. The experiments with pyridine showed that, with the faster diffusing initiator, the polymerization location was entirely outside the substrate. By selecting an appropriate anionic initiator, one with an appropriate diffusivity under the chosen reaction conditions, the location of the polymerization should be controllable. An initiator that diffuses out of the substrate faster than triphenylphosphine but slower than pyridine should produce a more surface-stratified composite. An investigation of different intiators and different monomers (e.g., butyl 2-cyanoacrylate) would be a logical next step to this research.

Still, with enough PECA incorporation, the composites showed an improvement in DCB cleavage tests. DCB cleavage tests are designed to test the integrity of substrate/adhesive joints. The reason for the improved performance of the composites was not due to increased adhesion between the substrate and the test adhesive (epoxy). Adding functional groups to the surface did not improve the performance of the composites. Mechanical integrity in the DCB tests was improved by enhancing of the cohesive strength of the substrate surface. Joints of pure FEP and epoxy are poor, not because of poor adhesion between the two materials: rather, the joints fail within the FEP either due to poor bulk cohesiveness or the existence of a weak surface later. The incorporation of PECA into FEP at high enough concentrations seems to enhance the cohesive strength of the material.

**Acknowledgment.** We thank the Office of Naval Research and the Green Polymer Chemistry Cluster of the Center for UMass−Industry Research on Polymers for financial support. We also thank the NSF-funded UMass Materials Research Science and Engineering Center for use of the central facilities.

## References and Notes

(1) Watkins, J. J.; McCarthy, T. J. *Macromolecules* **1994**, *27*, 4845.
(2) Watkins, J. J.; McCarthy, T. J. *Macromolecules* **1995**, *28*, 4067.
(3) Kung, E.; Lesser, A. J.; McCarthy, T. J. *Macromolecules* **1998**, *31*, 4160.
(4) Pepper, D. C. *J. Polym. Sci., Polym. Symp.* **1978**, *62*, 65.
(5) Shantha, K. L.; Thennarasu, S.; Krishnamurti, N. *J. Adhes. Sci. Technol.* **1989**, *3*, 237.
(6) Odian, G. *Principles of Polymerization*, 3rd ed.; John Wiley & Sons: New York, 1991.
(7) Johnston, D. S.; Pepper, D. C. *Makromol. Chem.* **1981**, *182*, 393.
(8) Donnelly, E. F.; Johnston, D. S.; Pepper, D. C. *J. Polym. Sci., Polym. Lett. Ed.* **1977**, *15*, 399.
(9) Woods, J.; Guthrie, J.; Rooney, J.; Kelly, L.; Doyle, A.; Noonan, E. *Polymer* **1989**, *30*, 1091.
(10) Fawcett, A. H.; Guthrie, J.; Otterburn, M. S.; Szeto, D. Y. S. *J. Polym. Sci., Part C: Polym. Lett.* **1988**, *26*, 459.
(11) Pepper, D. C. *Polym. J.* **1980**, *12*, 629.
(12) Johnston, D. S.; Pepper, D. C. *Makromol. Chem.* **1981**, *182*, 407.
(13) Pepper, D. C.; Ryan, B. *Makromol. Chem.* **1983**, *184*, 395.
(14) Pepper, D. C.; Ryan, B. *Makromol. Chem.* **1983**, *184*, 383.
(15) Gordon, A. J.; Ford, R. A. *The Chemist's Companion*; John Wiley & Sons: New York, 1972.
(16) Jaffe, H. H.; Freedman, L. D. *J. Am. Chem. Soc.* **1952**, *74*, 1069.
(17) Feiring, A. E. In *Organofluorine Chemistry*; Banks, R. E., Smart, B. E., Tatlow, J. C., Eds.; Plenum Press: New York, 1994; pp 339−372.
(18) Williams, J. G. *Fracture Mechanics of Polymers*; Halsted Press: New York, 1984.

MA000695O